# Oxidation Kinetics for Ni(111) and the Structure of the Oxide Layers

**T. Okazawa, T. Nishizawa, T. Nishimura, and Y. Kido***

**Abstract**

The oxidation kinetics for Ni(111) surface and the structure of the oxide layers grown at room temperature were analyzed by high-resolution medium energy ion scattering using isotopically labeled $^{18}O_2$. Initially, the surface showed a RHEED(reflection high energy electron diffraction) pattern of the Ni(111)-(2×2)-O chemisorption structure at an oxygen exposure of a few Langmuir (1 L: $10^{-6}$ Torr s) and started to form NiO(111) layers above 10 L. The oxide thickness was saturated with six atomic layers at oxygen exposure of 160 L. The saturated NiO(111) surface showed a (1×1) RHEED pattern not *p*(2×2) and consists of two domains, NiO(111)-[$11\bar{2}$]//Ni(111)-[$11\bar{2}$](primary) and NiO(111)-[$1\bar{1}0$]// Ni(111)-[$11\bar{2}$](a small fraction). The elemental depth profile corresponds to the octopolar reconstruction terminated with Ni (0.25 ML) (1 ML = $1.33\times10^{15}$ atoms/cm$^2$: areal density of NiO(111)). The oxide surface grown epitaxially probably takes a precursor state of the octopolar structure with significant distortion because of a large lattice mismatch of 19 % between NiO(111) and Ni(111). Tow step oxidation using $^{18}O_2$ and $^{16}O_2$ clearly indicates that oxidation takes place at the top surface obeying the Cabrera-Mott mechanism. The potential barrier for the jump from Ni into the NiO layer is derived to be 2.36 eV.

---

*Department of Physics, Ritsumeikan University, Kusatsu, Shiga-ken 525-8577, Japan*

Polar rocksalt surfaces were long believed to be unstable because of a nominally infinite surface energy. In fact, it was experimentally evidenced that the clean surfaces facetted into neutral {100} type planes[1]. However, Wolf[2] predicted that the (111) surfaces of rocksalt crystals were stabilized by taking a *p*(2×2)-octopolar structure. Indeed, the *p*(2×2) structure was observed for the NiO(111) surfaces grown epitaxially on Au(111)[3,4] and on single crystal NiO(111)[4]. Rohr et al.[5] oxidized Ni(111) to form the NiO(111) surface and observed a diffused *p*(2×2) pattern for the surface after annealing that covered with hydroxyl groups. According to the report of Barbier et al.[4], the octopolar reconstruction formed on the single crystal NiO(111) takes a single Ni termination and that on NiO(111) thin films grown on Au(111) has both Ni and O terminations.

In this work, we oxidized the single crystal Ni(111) to grow epitaxially NiO(111) layers at room temperature(RT) and clarify the surface structure of the NiO(111) by means of high-resolution medium energy ion scattering (MEIS). In addition, analysis using isotopically labeled $^{18}O_2$ reveals the oxidation kinetics. The present MEIS analysis using a toroidal electrostatic analyzer (ESA) allows a layer-by-layer analysis[7]. The NiO(111) surface exhibits a (1×1) RHEED (reflection high energy electron diffraction) pattern not the *p*(2×2) but takes a layered structure of Ni(0.25 ML)/O(0.75 ML)/NiO(111) suggesting a octopolar-like structure terminated with Ni. Here, 1 ML (monolayer) is defined as the areal density of the NiO(111) plane ($1.33\times10^{15}$ atoms/cm$^2$). The oxidation kinetics of Ni has been studied for a long time in terms of the Cabrera-Mott oxidation mechanism[6]. In this study, we clearly evidence that Ni ions are transported to the surface and oxidation takes place at the top surface.

We prepared the clean surface of a single crystal Ni(111) by repetition of sputtering with 0.75 keV $Ar^+$ and annealing at 650°C under ultra-high vacuum (UHV) condition. The RHEED observation showed a clear (1×1) pattern (see Fig. 1(a)) and no surface contaminations were confirmed by MEIS using 120 keV $He^+$ ions under a double alignment condition ([011]-incidence and $[21\bar{1}]$-emergence). The clean surface was then exposed to $O_2$ at a pressure ranging from $1\times10^{-8}$ to $1\times10^{-6}$ Torr at RT. At an initial stage of oxidation with $O_2$-exposure from 1 to 3 L the surface showed a (2×2)-RHEED pattern (see Fig.1(b)) indicating oxygen chemisorption[8-10]. The NiO(111) phase starts to grow for $O_2$ exposure above 10 L (see Fig.1(c)) and oxidation was saturated at $O_2$-exposure of 160 L. As seen from the RHEED pattern(Fig.1(d)), the NiO(111) layer grows epitaxially and has two types of domains, NiO(111)-$[1\bar{1}0]$//Ni(111)-$[1\bar{1}0]$(primary) and NiO(111)-$[11\bar{2}]$//Ni(111)- $[1\bar{1}0]$ (a small fraction).

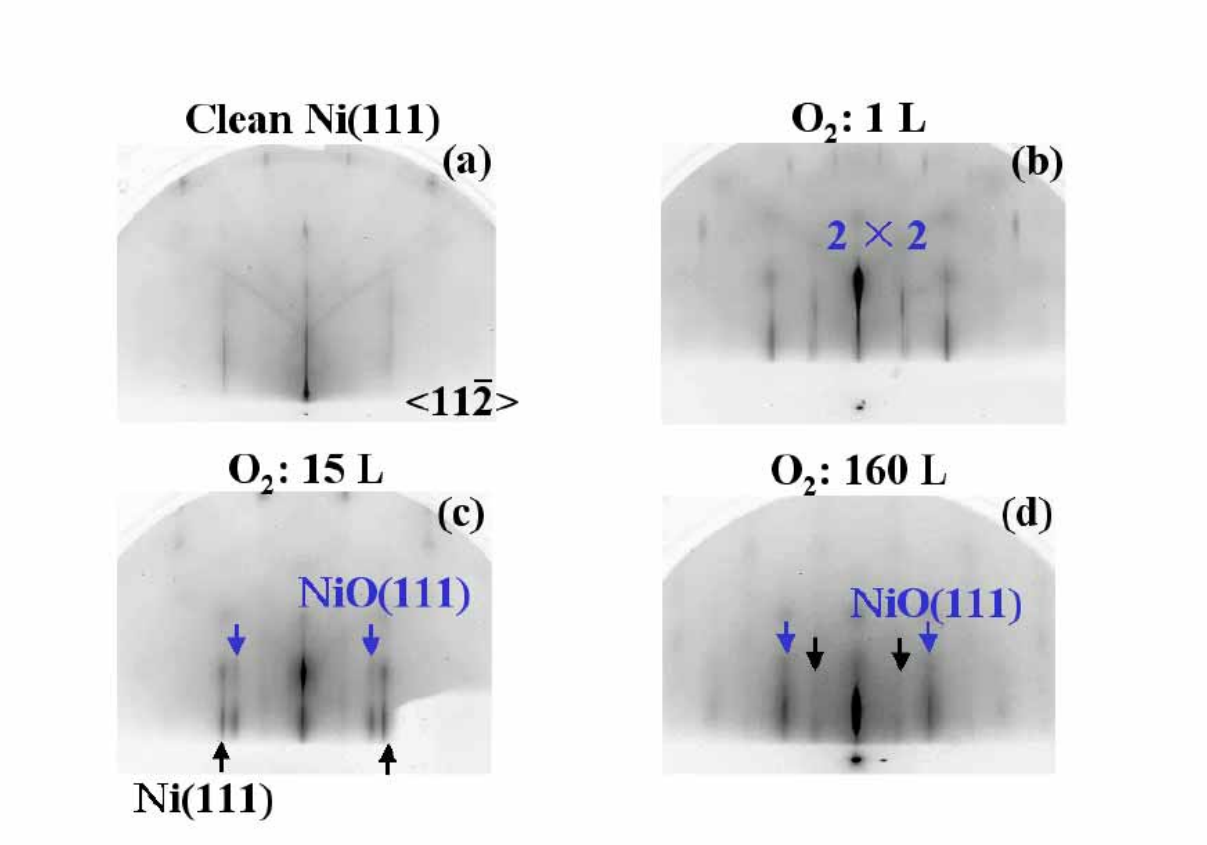


FIG. 1. RHEED patterns observed for clean Ni(111) surface (a), oxidized with $O_2$-exposure of 1 L (b), 15 L (c), and 160 L (d). Here, 30 keV electron beams were incident along the [$11\bar{2}$]-axis of Ni(111).

Figure 2(a) shows the MEIS spectra observed for the Ni(111) surfaces oxidized at RT for $O_2$-exposure of 3, 15, 50, and 160 L. The solid curves are the simulated spectra best-fitted to the observed ones assuming the depth profiles indicated in Fig. 2(b). The growth mode is not in a layer-by-layer fashion. With increasing oxygen exposure, the oxidation rate drastically drops. The saturated oxygen and nickel coverage was estimated to be $3.9\pm0.05\times10^{15}$ and $4.1\pm0.04\times10^{15}$atoms/cm$^2$, respectively, corresponding to about three NiO(111)-double layers, O(1 ML)/Ni(1 ML)/O(1 ML)/Ni(1 ML)/O(1 ML)/Ni(1 ML) on Ni(111). In order to estimate precisely the absolute amounts of O and Ni, it is essential to determine the $He^+$ fractions dependent on atomic species of scatterer and the emerging velocity and angle[11]. Here, it must be noted that the toroidal ESA detected $He^+$ ions only. The $He^+$ fractions were determined in advance using poly crystals of $SiO_2$ and Ni films and a NiO(001) single crystal. Another important factor to determine absolute amounts of composite elements is the scattering cross sections, which were calculated from the ZBL potentials[12].

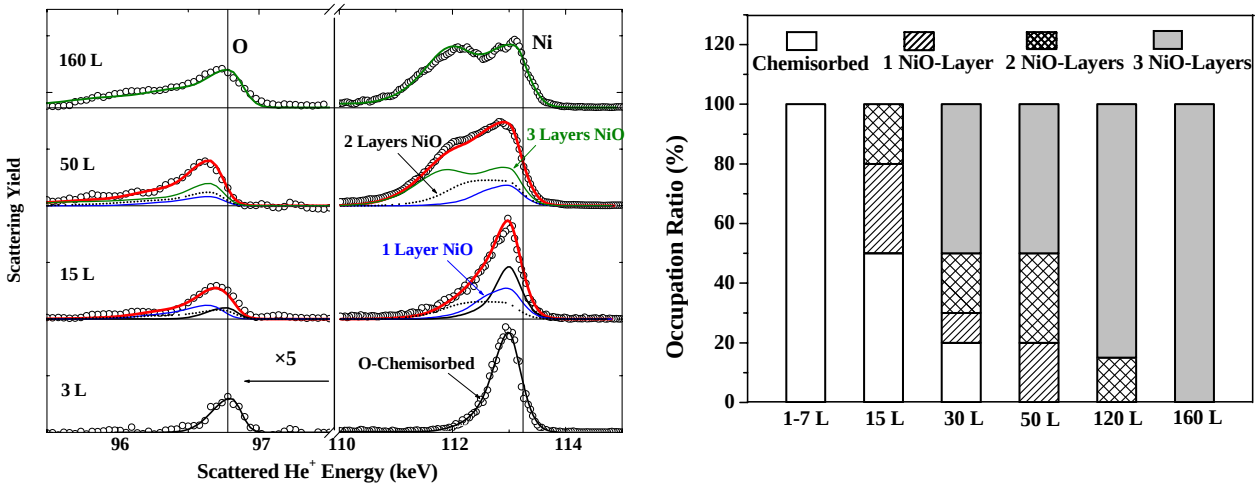


FIG. 2 (a) MEIS spectra observed for the Ni(111) surfaces oxidized at RT for $O_2$-exposure of 3, 15, 50, and 160 L. 120 keV $He^+$ ions were incident along the [001] axis and backscattered to 70.0° with respect to surface normal. The vertical lines indicate the energy positions for $He^+$ ions backscattered from O and Ni atoms on top surface. The solid curves are the simulated MEIS spectra best-fitted to the observed ones assuming the elemental depth profiles, which are indicated in Fig. 2 (b).

In order to analyze the fine structure of the top surface, we performed the MEIS analysis taking a glancing emergence geometry, where 120 keV $He^+$ ions were incident along the [001] axis and backscattered to 85.0° with respect to surface normal. Figure 3 shows the MEIS spectra, in which the scattering component from each atomic layer is clearly resolved.

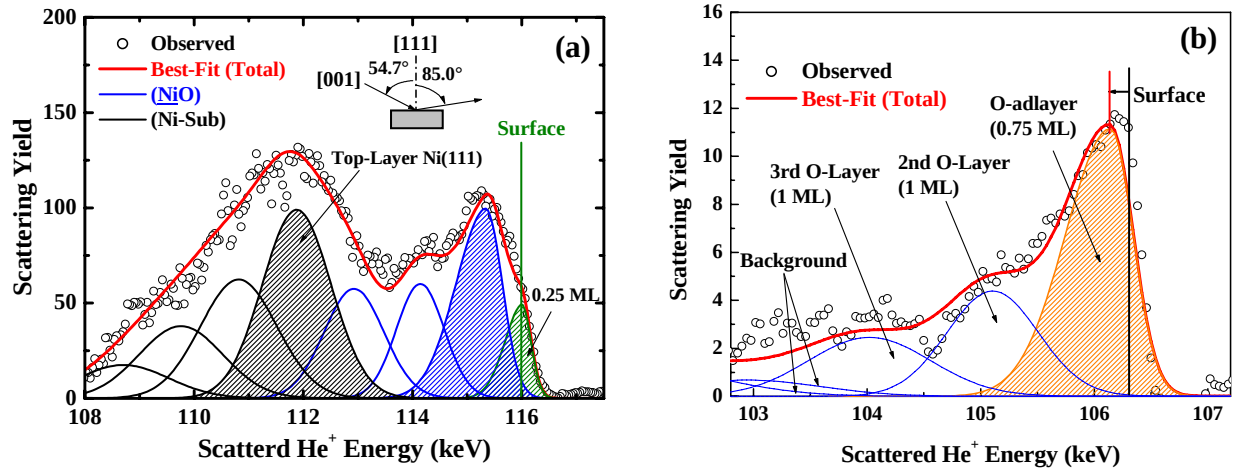


FIG. 3. MEIS spectra observed for the Ni(111) surface oxidized with $O_2$-exposure of 160 L. Scattering components from Ni (a) and from O (b). Scattering geometry was set to [001]-incidence

and backscattering to 85.0° with respect to surface normal. The solid curves denote the simulated MEIS spectra giving the best-fit to the observed ones assuming the elemental depth profile of Ni(0.25 ML)/O(0.75 ML)/Ni(1 ML)/O(1 ML)/Ni(1 ML)/O(1 ML)/Ni(1 ML)/Ni(111).

As a result, it is seen that the topmost layer consists of 0.25±0.03 ML Ni sitting on the O-plane (0.75±0.04 ML). The underlying Ni/O/Ni/O/Ni layers were significantly shadowed, because the domain of NiO(111)-[$1\bar{1}0$]//Ni(111)-[$1\bar{1}0$] is dominant. It must be noted that top layer Ni(111) is visible for the $He^+$ ions incident along the [001] axis but the underlying Ni(111) layers are shadowed. The adatoms (Ni(1/4 ML)) and adlayer (O(3/4 ML)) are located on the bulk-truncated NiO(111) with thickness of five atomic layers on the Ni(111) substrate. Such a surface structure coincides with the octopolar reconstruction terminated with Ni (see Fig. 4). However, the present NiO(111) surface grown on Ni(111) showed the (1×1) RHEED pattern not the *p*(2×2) image. This is probably due to some stress imposed by the underlying thin NiO(111) layer, which may be caused by a large lattice mismatch of 18 % between NiO(111) and Ni(111). This adatoms-adlayer structure may correspond to a precursor state of the *p*(2×2)-octopolar reconstruction. Here, it must be noted that the clear *p*(2×2) pattern was observed for NiO(111) single crystal[4] and NiO(111) films grown epitaxially on Au(111)[3,4] (the lattice mismatch between NiO(111) and Au(111) is 2 %).

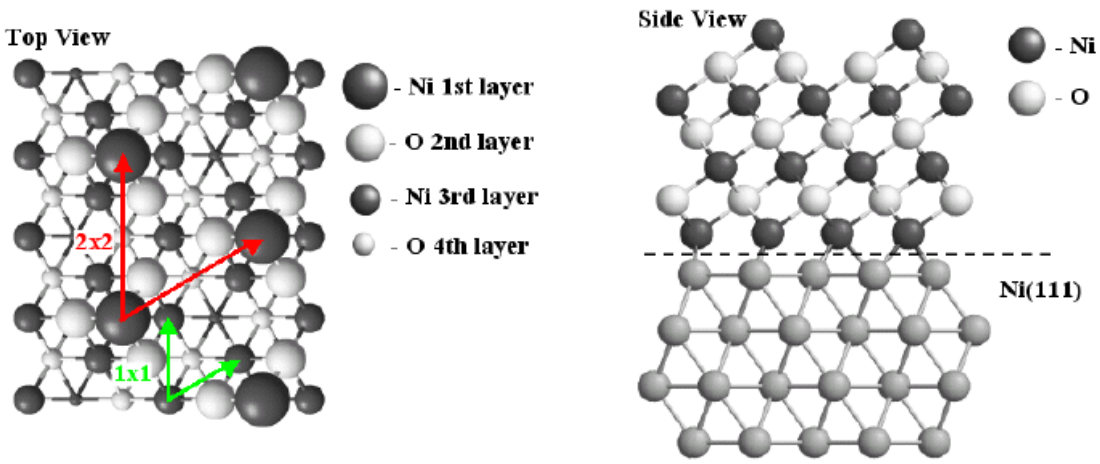


FIG. 4. Top and side views of octopolar reconstruction terminated with Ni.

Next, we analyzed the oxidation kinetics using isotopically labeled $^{18}O_2$ (purity: 95 %) and $^{16}O_2$. The clean Ni(111) surface was first oxidized in $^{18}O_2$ at RT with an exposure of 20 L. The average thickness of the Ni$^{18}$O(111) is estimated to be about 2.9 atomic layers derived from MEIS analysis (see Fig. 5(b)). Then the surface was reoxidized in $^{16}O_2$ at RT with an exposure of 140 L. Figure 5(a) shows the MEIS spectra observed for the NiO(111)/Ni(111) oxidized in $^{18}O_2$ (top) and that

re-oxidized in $^{16}O_2$ (bottom). The simulated MEIS spectra best-fitted to the observed ones give the elemental depth profiles, as indicated in Fig. 5(b). Apparently, Ni atoms(ions) diffuse to the surface and the oxidation takes place on the top surface. The average thickness of the re-oxidized NiO(111) layer is estimated to be 3.1 atomic layers. According to the Cabrera-Mott model[13], for a thin oxide film (less than 3 nm), electrons tunnel from a metal to an adsorbed oxygen atom through a dielectric film (oxide film) in order to equalize the electrochemical potential. This creates an electric field across the oxide film, which in turn allows metal ion transport to the top surface. A dissolved $Ni^+$ ion jumps to the oxide layer against a potential barrier ($W$) and then drifts to the top surface. The drift velocity $u$ is limited by the barrier height and thus expressed by

$$u = N\Omega \, \nu \exp[-W / k_B T] , \qquad (1)$$

where $N$, $\Omega$, $\nu$, $k_B$, and $T$ are the areal density of the dissolved $Ni^+$, the volume per one $Ni^+$, frequency of thermal lattice vibration, Boltzmann constant, and temperature, respectively. The growing oxide thickness $X$ on time $t$ is expressed by

$$\frac{X_L}{X^2} u \; t = \exp[-\frac{X_L}{X}] , \qquad (2)$$

where $X_L$ is a constant (2 nm for oxidation of Ni[6]). If the Cabrera-Mott model is applied to the above re-oxidation in $^{16}O_2$ after oxidation in $^{18}O_2$, one obtains the potential barrier $W$ of 2.36 eV. Here, we used the average thickness of the re-oxidized NiO(111) $X = 3.73\times10^{-8}$ cm, $\nu = \nu_D$ (= $9\times10^{12}$ $s^{-1}$ : Debye cut-off frequency), $N\Omega = 2.035\times10^{-8}$ cm, $k_BT = 0.03$ eV, and $t = 1400$ s. This is consistent with the previous prediction (2.56 eV) based on the Cabrera-Mott model[6].

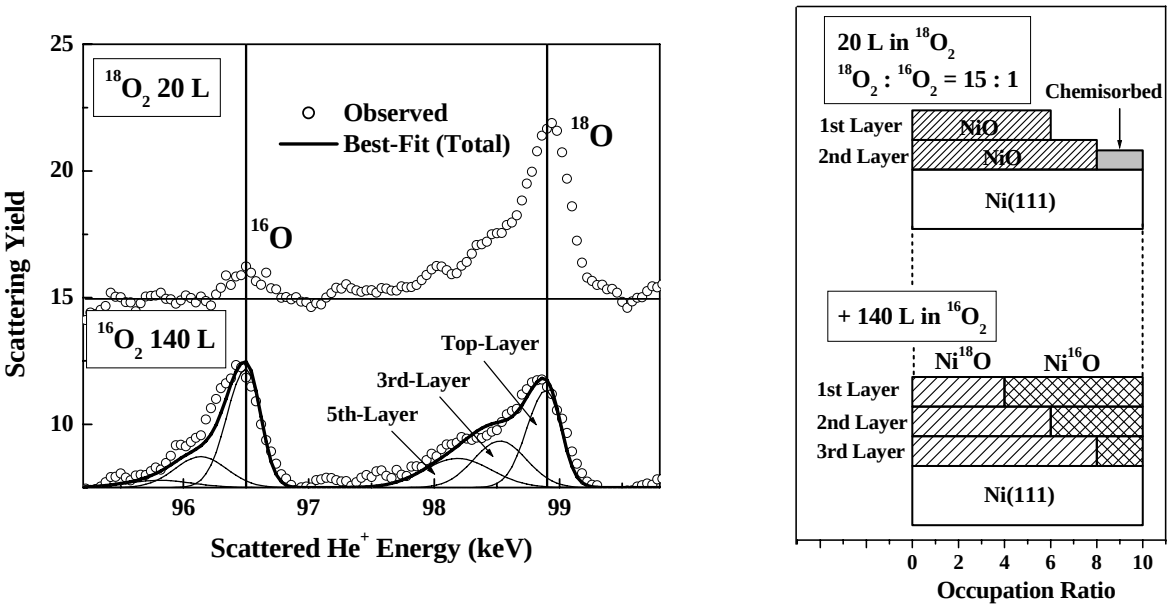


FIG. 5. MEIS spectra observed for the NiO(111)/Ni(111) oxidized in $^{18}O_2$ with an exposure of 20 L(upper) and that reoxidized in $^{16}O_2$ with an exposure of 140 L(bottom). The scattering geometry

takes the [100]-incidence and backscattering to 70.0° with respect to surface normal. Best-fit was obtained assuming the elemental depth profiles, indicated schematically in Fig. 5(b). For exposure to $^{18}O_2$(20 L), the surface covered with three kinds of domains with different thickness, 4 atomic-layers of NiO(60 %), 2 atomic-layers of NiO(20 %), and O-chemisorbed(20%). For exposure to $^{16}O_2$(140 L), oxidation is saturated with the depth profile of Ni(0.25 ML)/O(0.75 ML)/Ni(1 ML)/O(1 ML)/Ni(1 ML)/O(1 ML)/Ni(1 ML)/Ni(111).

In summary, the oxidation kinetics for Ni(111) surface and the structure of the oxide layers grown epitaxially at RT were analyzed by high-resolution MEIS using isotopically labeled $^{18}O_2$. Initially, the surface showed a RHEED pattern of the Ni(111)-(2×2)-O chemisorption structure at an oxygen exposure of a few L and started to form NiO(111) layers above 10 L. The growth mode is not in a layer-by-layer fashion. The oxide thickness was saturated with six atomic layers at oxygen exposure of 160 L. The saturated NiO(111) surface showed a (1×1) RHEED pattern not *p*(2×2) and consists of two domains, NiO(111)-[ $11\bar{2}$ ]//Ni(111)-[ $11\bar{2}$ ] (primary) and NiO(111)-[$1\bar{1}0$]//Ni(111)-[$11\bar{2}$] (a small fraction). The elemental depth profile corresponds to the octopolar reconstruction terminated with Ni(0.25ML). The oxide surface grown epitaxially probably takes a precursor state of the octopolar structure with significant distortion because of a large lattice mismatch of 19 % between NiO(111) and Ni(111). Tow step oxidation using $^{18}O_2$ and $^{16}O_2$ clearly indicates that oxidation takes place at the top surface obeying the Cabrera-Mott mechanism. The potential barrier for the jump from Ni into the NiO layer is derived to be 2.36 eV, which is compatible with the previously predicted value of 2.56 eV for migration of Ni ions through the NiO lattice.

**Acknowledgements**

This work was supported partly by Japan Science and Technology Agency, JST, CREST.

**References**

1. V.E. Henrich, Surf. Sci. **57**, 385 (1976).
2. D. Wolf, Phys. Rev. Lett. **68**, 3315 (1992).
3. C.A. Ventrice, Jr., Th. Bertrams, H. Hannemann, A. Brodde, and H. Neddermeyer, Phys. Rev. **B 49**, 5773 (1994).
4. A. Barbier, C. Mocuta, H. Kuhlenbeck, K.F. Peters, B. Richter, and G. Renaud, Phys. Rev. Lett. **84**, 2897 (2000).
5. F. Rohr, K. Wirth, J. Libuda, D. Cappus, M. Bäumer, and H.-J. Freund, Surf. Sci. **315**, L977

(1994).
6. A. Atkinson, Rev. Mod. Phys. **57**, 437 (1985).
7. Y. Kido, T. Nishimura, Y. Hoshino, and H. Namba, Nucl. Instrum. Methods **B161/163**, 371 (2000).
8. T. Narusawa and W.M. Gibson, Surf. Sci. **114**, 331 (1982)
9. D.F. Michell and M.J. Graham, Surf. Sci. **114**, 546 (1982).
10. P. Dolle, M. Alnot, J.J. Ehrhardt, A. Thomy, and A. Cassuto, Surf. Sci. **152/153**, 620 (1985).
11. T. Nishimura, Y. Hoshino, and Y. Kido, Surf. Sci. **452**, 139 (2000).
12. J.F. Ziegler, J.P. Biersack, and W. Littmark, *The Stopping and Range of Ions in Matter* (Pergamon, New York, 1985).
13. N. Cabrera and N.F. Mott, Rep. Prog. Phys. **12**, 163 (1948-1949).